# Distribution of Ligand Field Strength. Generation by Mechanical Stressing, Its Consequences and Technical Application

MAMORU SENNA

*Faculty of Science and Technology, Keio University, Hiyoshi, Yokohama, 223-8522 (Japan)*

*E-mail: senna@applc.keio.ac.jp*

## Abstract

Deformed molecules exhibit anomaly in various aspects. Mechanical stressing, being anisotropic in nature, on the molecular crystals inevitably brings about quenched deformation of constituent molecules. When we deal with coordination compounds, deformation of the molecule results in disproportionation of ligands to change them into asymmetric, and hence develops distribution of ligand field strength. Consequences of introducing such asymmetry are very diverse. Gradual spin crossover and substitution of ligands by counter ions are only a few examples. Solid state ligand exchange is particularly of importance, since this opens up a new way for synthesizing various coordination compounds using neither solvents nor catalysts. Evidences of distribution of ligand field strength are shown for ferrous coordination compounds. Subsequently, application to the synthesis of some ferrous pyridyl compounds is demonstrated.

## INTRODUCTION

Most of the chemical principles rest upon symmetry, basically due to symmetry of the electronic orbitals [1]. Although different factors, geometry, and electron localization, are also involved, crystallographical properties are dominated by the symmetry principle. Mechanochemistry is distinct from many other athermal processes like photo-, irradiation or electrochemistry in the sense that mechanical stress on the solid can produce off-symmetry of the atomic arrangement. When we deal with inorganic crystals, what we observe is the disturbance of crystal field symmetry, leading to formation of heterobridging bonds [2]. However, distortion of molecules is by far influential in the body of the chemical reaction, in which no other manipulation can achieve.

It is particularly interesting to examine the changes in the properties of metal coordinate compounds in a solid state under mechanical stressing because there are many well-defined theoretical bases for those compounds. On top of that, there are many convenient methods for characterization like vibrational spectroscopies (*e. g.*, IR, UV-vis), magnetic resonance spectroscopy (*e. g.*, NMR, EPR) or magnetic properties by SQUID magnetometer.

Mechanochemistry of coordination compounds is also attractive in view of the practical application because of its optical and magnetic properties. In this feature article, the author tries to present concept and consequences of ligand field distortion and its distribution, based mainly on the recent research works in his laboratory.

## LIGAND FIELD DISTORTION AND ITS DISTRIBUTION

When mechanical stress is exerted on coordination compounds in a solid state, their constituent molecules are subject to distortion. The manner and the extent of the distortion depend on the molecular species, and the strength and anisotropy of the exerted mechanical stress. The distortion of the molecules causes, in turn, a change in the strength and anisotropy of the ligand field. Such a change in the ligand field leads to a considerable modification of magnetism and reactivity [3, 4].

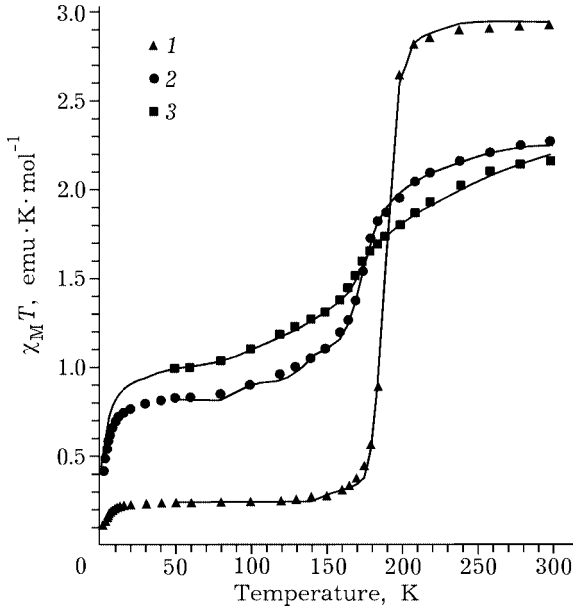


Fig. 1. Temperature dependence of observed values of $c_M T$ for $Fe^{II}(phen)_2(NCS)_2$: *1* – intact; *2* – after milling for 1 h, and *3* – after milling for 5 h; the solid curves denote values calculated by eq (1).

Electronic configuration of divalent iron ion, $Fe^{II}$, in a octahedrally coordinated state is either low spin (LS, $^1A_{1g}$; $t_{2g}^6 e_g^0$), or high spin (HS, $^5T_{2g}$; $t_{2g}^4 e_g^0$), depending on the ligand field strength, D, and the spin pairing energy, $P$ [5–8]. Spin transition from LS to HS occurs when $|D - P|$ becomes comparable to the thermal energy. The transition is accompanied by changes in the intramolecular conformation [5–9]. This is attributed to the presence of two electrons in the $e_g$ orbitals which enhance the repulsive component of the $Fe^{II}$-ligand bonding to a higher extent than the $t_{2g}$ orbitals.

Ligand field distortion and its distribution are visualized by the change in the spin crossover behavior. For example, the persistence of molecules in HS state below the original spin crossover temperature and broadening of the transition temperature were reported for mechanically stressed $Fe^{II}(phen)_2(NCS)_2$ [9], $Fe^{II}(bt)_2(NCS)_2$ (bt = 2,2'-bi-2-thiazoline) [10] and

TABLE 1

Thermodynamic parameters of spin states for $Fe^{II}(phen)_2(NCS)_2$ without or with milling

| Sample | $i$ | $c_i$ | $T_{1/2,i}$, K | $\Delta H_i$, kJ ×mol$^{-1}$ | $\Delta S_i$, J ×mol$^{-1}$ ×K$^{-1}$ | $n_i$ | $[dc_M T/dT]_{max}$[c], emu × mol$^{-1}$ |
|---|---|---|---|---|---|---|---|
| Intact | LS[a] | – | – | – | – | – | |
| | 1 | 0.00 | 270 | – | – | – | |
| | 2 | 0.02 | 230 | 11.2 | 48.8 | 6.0 | |
| | 3 | 0.75 | 190 | 9.3 | 48.8 | 7.4 | 0.144 |
| | 4 | 0.02 | 150 | 7.8 | 48.8 | 6.5 | |
| | 5 | 0.00 | 110 | – | – | – | |
| | HS[b] | 0.21 | – | – | – | – | |
| Milled for 1 h | LS[a] | 0.06 | – | – | – | – | |
| | 1 | 0.03 | 255 | 12.4 | 48.8 | 3.1 | |
| | 2 | 0.05 | 215 | 10.5 | 48.8 | 3.1 | |
| | 3 | 0.29 | 175 | 8.5 | 48.8 | 4.3 | 0.033 |
| | 4 | 0.05 | 135 | 6.6 | 48.8 | 4.3 | |
| | 5 | 0.03 | 95 | 4.7 | 48.8 | 4.0 | |
| | HS[b] | 0.49 | – | – | – | – | |
| Milled for 5 h | LS[a] | 0.07 | – | – | – | – | |
| | 1 | 0.05 | 250 | 12.2 | 48.8 | 3.1 | |
| | 2 | 0.08 | 210 | 10.2 | 48.8 | 3.1 | |
| | 3 | 0.13 | 170 | 8.3 | 48.8 | 4.0 | 0.015 |
| | 4 | 0.08 | 130 | 6.3 | 48.8 | 1.3 | |
| | 5 | 0.05 | 90 | 4.4 | 48.8 | 1.0 | |
| | HS [b] | 0.54 | – | – | – | – | |

[a]Fraction of the residual LS state. The component does not exhibit spin transitions.
[b]Fraction of the residual HS state. The value is calculated from the value of $c_M T$ at 50 K.
[c]Maximum value of slope in calculated $c_M T$ curves.

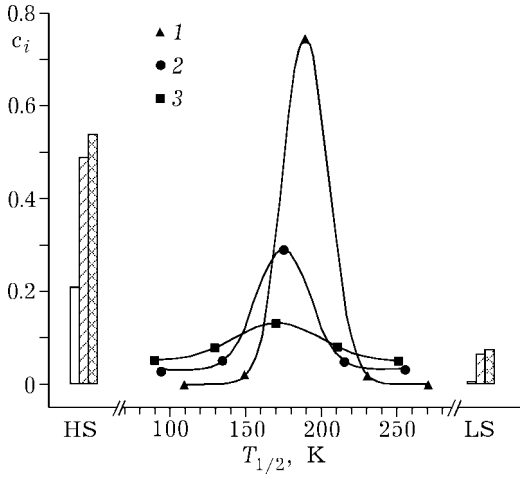


Fig. 2. Variation of fraction in the $i$-th component ($c_i$) with spin transition temperature ($T_{1/2}$) for $Fe^{II}(phen)_2(NCS)_2$: *1* – intact; *2* – after milling for 1 h, and *3* – after milling for 5 h; the values of $c_{HS}$ and $c_{LS}$ are represented by bars. Blanc, intact; dotted, after milling for 1 h; and striped, after milling for 5 h.

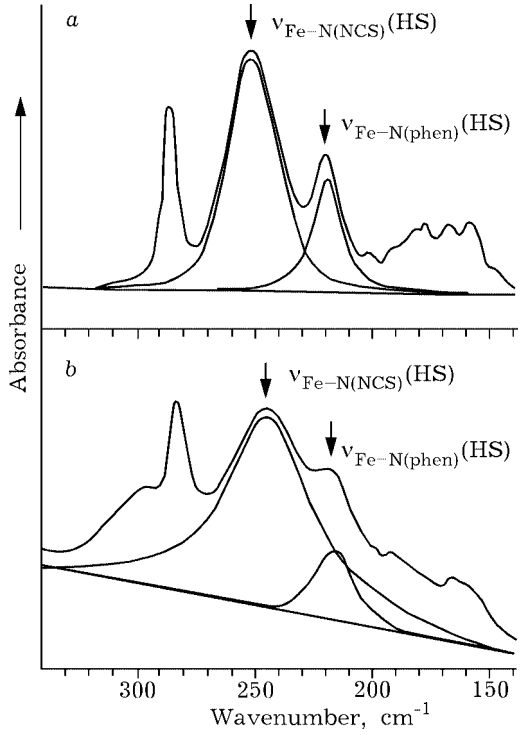


Fig. 3. Far-IR spectra of $Fe^{II}(phen)_2(NCS)_2$: *a* – intact, and *b* – after milling for 1 h.

$[Fe^{III}(X - SalEen)_2]PF_6$ (X – SalEen is mono-anion of the condensation product of salicylaldehyde or a methoxy-substituted salicylaldehyde and *N*-ethyl – ethylenediamine) [11, 12].

Figure 1 demonstrates the temperature dependence of the effective magnetic moment, $\mu_{eff}$, or of the molar magnetic susceptibility, $\chi_M$, multiplied by the temperature, $T$, by exerting mechanical stress on the coordination compound, $Fe^{II}(phen)_2(NCS)_2$ (phen = 1,10-phenanthroline) [13]. Note that $\chi_M T$ is proportional to $\mu^2_{eff}$. The change of the magnetic properties is primarily associated with the change in the electronic properties.

The change in the spin crossover behaviour is analyzed by the principle of multi-component fitting [5, 14, 15]. The principle, explained elsewhere in detail [14], rests upon the polynomial expression of the overall $\chi_M T$:

$$\chi_M T = [(N_0\mu_0)\,(3k_B)]\Sigma c_i[(1 - f_{HS,i})\,\mu^2_{LS} + f_{HS,i}\mu_{HS}{}^2] + (\chi_M T)_{50} \quad (1)$$

where $k_B$ is the Boltzmann constant, $R$ is the gas constant, $N_0$ is Avogadro number, and $\mu_0$ is the permeability of vacuum. The terms $\mu_{LS}$ and $\mu_{HS}$ correspond to the magnetic moments for the LS and the HS states, respectively. The HS state fraction of the $i$-th component, $f_{HS,i}$,

TABLE 2

Parameters of Mossbauer spectra of $Fe^{II}(phen)_2(NCS)_2$ without or with milling

| Sample | | $\delta$[a], mm ×$s^{-1}$ | $\Delta E_Q$[b], mm ×$s^{-1}$ | $\Gamma$[c], mm ×$s^{-1}$ | Peak area fraction | Spin state |
|---|---|---|---|---|---|---|
| intact | | 0.97 | 2.61 | 0.31 | 0.66 | HS |
| | | 0.23 | 0.33 | 0.35 | 0.34 | LS |
| milled for | 1h | 0.99 | 2.61 | 0.27 | 0.40 | HS |
| | | 0.27 | 0.29 | 0.50 | 0.60 | LS |
| | 5h | 0.97 | 2.57 | 0.31 | 0.36 | HS |
| | | 0.28 | 0.28 | 0.52 | 0.64 | LS |

[a]isomer shift.
[b]quadrupole splitting.
[c]half width at half maximum (FWHM) of Mössbauer absorption peak.

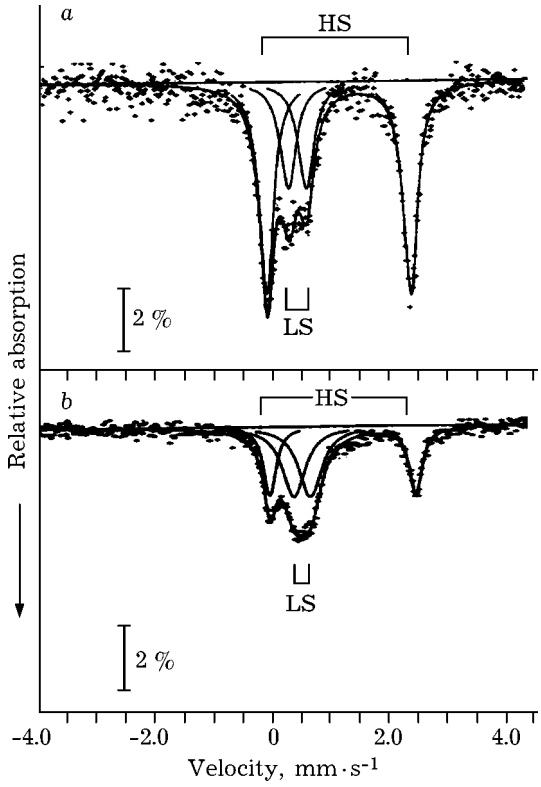


Fig. 4. Mössbauer spectra of $Fe^{II}(phen)_2(NCS)_2$: *a* – intact, and *b* – after milling for 1 h.

depends on the enthalpy, $\Delta H_i$, and the entropy, $\Delta S_i$, of the LS to HS transition, and also on the number of molecules per domain, $n_i$, as

$$f_{HS,i} = \{1 + \exp [n_i(\Delta H_i/(RT) - \Delta S_i/R)]\}^{-1} \quad (2)$$

The median spin transition temperature, $T_{1/2,i}$, is defined as

$$T_{1/2,i} = \Delta H_i/\Delta S_i \quad (3)$$

Results of the multicomponent analysis for $Fe^{II}(phen)_2(NCS)_2$ are summarized in Table 1. After milling, the fractions of the tail components, 1 and 5 become significant and $T_{1/2}$ and

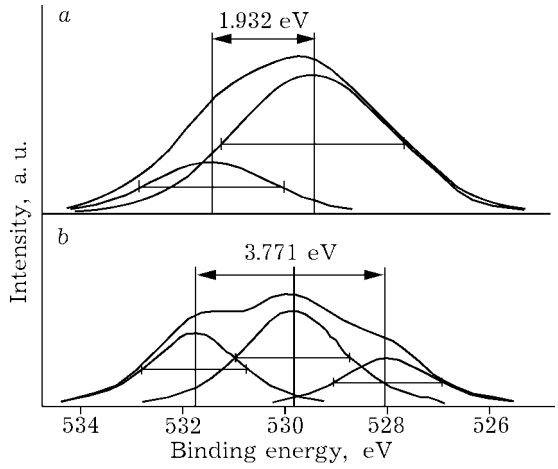


Fig. 5 X-ray photoelectron spectra of O 1*s* orbital of intact (*a*), and 3 h-milled (*b*) $FeCl_2 \times 4H_2O$.

the fraction of the main component 3 decreases, while the fraction of the residual HS state, $c_{HS}$, increases. The fraction of residual LS state, $c_{LS}$, also becomes significant. The fitting for the intact sample becomes fairly good, as shown in Fig. 1 by a solid line.

The maximum value of the derivative, $[dc_M T/dT]_{max}$, calculated from the fitting curve serves as a measure of the temperature sensitivity of spin crossover. Note that $[dc_M T/dT]_{max}$ is rapidly decreased in an early stage of milling. Fractional distribution of the spin crossover component, $c_i$, is plotted against $T_{1/2,i}$ in Fig. 2, where the solid lines denote the best-fit Gaussian curves. The distribution curve becomes broader with increasing milling time, most remarkably in 1 h.

Ligand field distribution is associated with the broadening of various spectra. One of the typical examples is the change in the IR spectra, as shown in Fig. 3, where increase in the peak width, $\Delta W$, relative to that for the intact sample

TABLE 3

Parameters of X-ray photoelectron spectra of O 1*s* orbital of $FeCl_2 \times 4H_2O$

| Sample | | Energy, eV | Intensity, a.u. | FWHM[a], eV | Fractional intensity |
|---|---|---|---|---|---|
| Intact | O1 | 527.8 | 1.94 | 1.06 | 0.15 |
| | O2 | 529.4 | 4.92 | 1.19 | 0.43 |
| | O3 | 531.1 | 4.15 | 1.36 | 0.42 |
| Milled for 3 h | O1 | 528.0 | 2.14 | 1.00 | 0.19 |
| | O2 | 529.8 | 4.65 | 1.18 | 0.50 |
| | O3 | 531.8 | 3.37 | 1.03 | 0.31 |

[a]Full width at half maximum.

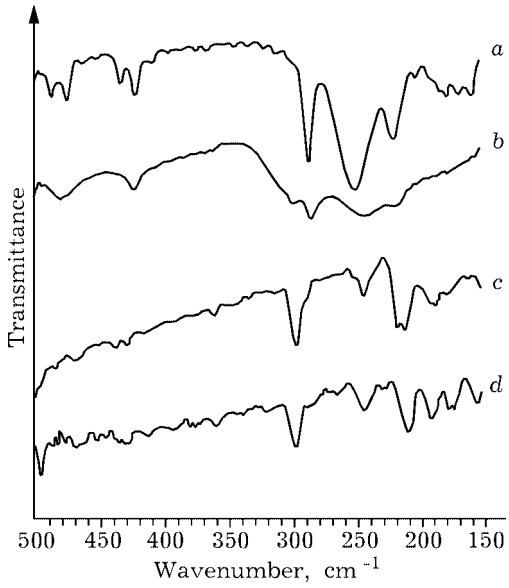


Fig. 6 Far-IR spectra of $Fe^{II}(phen)_2(NCS)_2$ (*a*, *b*) and $[Fe^{II}(phen)_3(PF_6)_2]$ (*c*, *d*):
*a*, *c* – intact, and *b*, *d* – after milling for 5 h.

is remarkable for the Fe–N(NCS) peak, observed at around 249 $cm^{-1}$. Similar broadening is observed in Mössbauer spectra by milling. Not only the fraction of LS increases, but also the FWHM increases as well by milling, as shown in Fig. 4. The related values are summarized in Table 2.

#### DISPROPORTIONATION OF LIGANDS

Distortion and distribution of ligand field just described above results further in the disproportionation of the ligands. This in turn brings about enormous change in the reactivity, since most of the reactions of coordination compounds are rationally regarded as those of ligand exchange. As a consequence of milling $FeCl_2 \times 4H_2O$, the peak profile of O1*s* binding energy determined by X-ray photoelectron spectroscopy changes remarkably, as shown in Fig. 5. Two components, O2 and O3, specified in Table 3, are attributed to two different kinds of water molecules coordinated to iron(II), according to the neighboring atoms [16]. On the other hand, the component O1 is due to adsorbed water molecules. While the component O1, in the lowest energy side exhibits no eventual peak shifts, two other O1*s* components, O2 and O3, shift toward the higher energy side. In addition, the proportion of O2 to O3 also changes to bias for O2 at lower energy to an appreciable extent. This suggests the change in the bonding state between iron and oxygen by milling, and also the disproportionation of the hydrated states of $H_2O$ molecules by milling. The consequence of the disproportionation is also straightforwardly reflected on the TG – DTA profiles [17].

#### MECHANOCHEMICAL LIGAND EXCHANGE

Prior to our trial to synthesize metal-organic coordination compounds directly *via* a mechanochemical route from a simple inorganic coordination compound and ligand species, we have observed several mechanochemical reactions between the ligand and the counterion [4]. As we milled $[Fe^{II}(phen)_3](NCS)_2 \times H_2O$ for instance, we observed a new peak in far-IR spectrum at 296 $cm^{-1}$, as shown in Fig. 6. This peak is close to those of phen vibration in the LS state of $Fe^{II}(phen)_2(NCS)_2$. This is a strong indication that some of the counterions, NCS, enter into the ligand field and replace phen. Milling $[Fe^{II}(phen)_3](PF_6)_2$ under the same condition, however, did not show any sign of ligand exchange. We attributed the difference to the smaller polarity and the larger volume

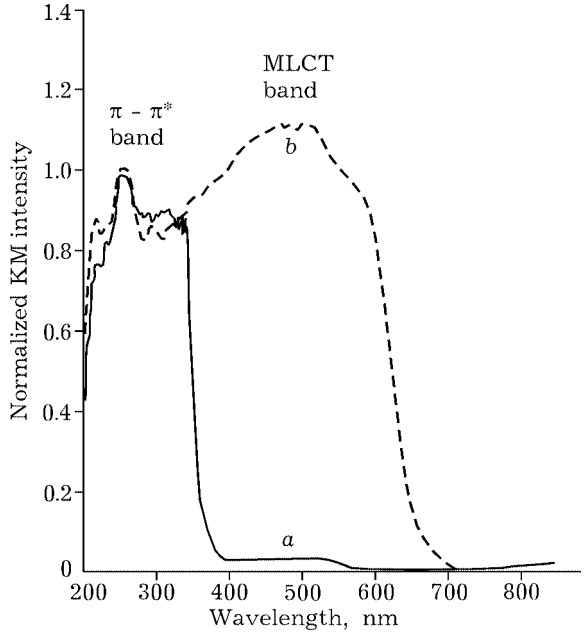


Fig. 7. UV-vis diffuse reflectance spectra of (*a*) as-mixed and (*b*) 3 h-milled mixture of $FeCl_2 \times 4H_2O$ and phen.

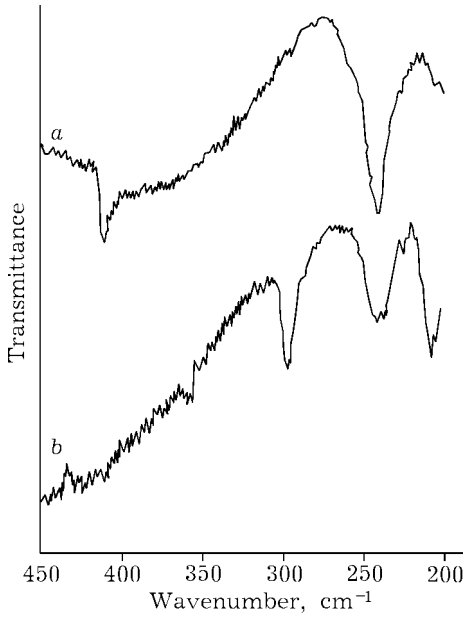


Fig. 8. Far-infrared absorption spectra of (*a*) as-mixed and (*b*) 3 h-milled mixture of $FeCl_2 \cdot 4H_2O$ and phen.

of $PF_6$ as compared to those of NCS, with smaller, linear conformation and appreciable permanent dipole moment. This speculation is, however, further to be confirmed by other possible components including the role of crystal water for the NCS compound.

Keeping in mind the mechanochemical ligand exchange reactions mentioned above, we further tried to synthesize $[Fe^{II}(phen)_3]Cl_2 \cdot \times nH_2O$ from $FeCl_2 \times 4H_2O$ and phen *via* a mechanochemical route [17]. As shown in Fig. 7, a strong absorption band at around 260 nm is observed in the UV-vis spectrum of the as-mixed sample (curve *a*). After milling, a broad absorption band peaked at around 500 nm appears and the peak intensity increases with milling time (curve *b*). Based on the reported assignment of $[Fe(phen)_3]^{2+}$ in solution [18], the band at around 260 nm is ascribed to p* ¬ p transition, and that at around 500 nm to metal to-ligand charge transfer (MLCT). The vertical axis of Fig. 7 is normalized so that the intensity of p* ¬ p peak at around 260 nm becomes unity. The appearance of MLCT band indicates the coordination of phen to the central iron(II), and hence, formation of $Fe^{II}$-phen coordination compounds.

This is in accordance with the IR results shown in Fig. 8. In a starting mixture, IR absorption bands are observed at 240 cm$^{-1}$ and 411 cm$^{-1}$ (curve *a*) due to the ring vibration of free phen ligand [19]. After milling for 3 h, new bands appear at 207, 297 and 358 cm$^{-1}$, as shown by curve *b*, while the band at 411 cm$^{-1}$ from free phen disappears. The band at 240 cm$^{-1}$ due to the ring vibration of free phen also disappears and a new band appears at 242 cm$^{-1}$. Based on the previous IR studies on the iron (II) complexes with phen ligands [19–21], we assign the band at 358 cm$^{-1}$ to the Fe–N(phen) stretching vibration and that at 207 cm$^{-1}$ to the N–Fe–N(phen) bending vibration for $[Fe(phen)_3]^{2+}$. The bands at 242 and 297 cm$^{-1}$ are ascribed to the phen ligand vibration activated by complex formation. These changes in the IR spectra by milling strongly suggest formation of the coordination compounds including $[Fe(phen)_3]^{2+}$ almost to completion, since the signals from the starting compounds entirely disappear.

We further examined the effects of preliminary milling of one of the reactants, $FeCl_2 \times 4H_2O$ in the hope that the deliberately introduced disproportionation of the 4 water molecules may accelerate the subsequent mechanochemical reaction. This was actually observed. As shown in Fig. 9, preliminary milling

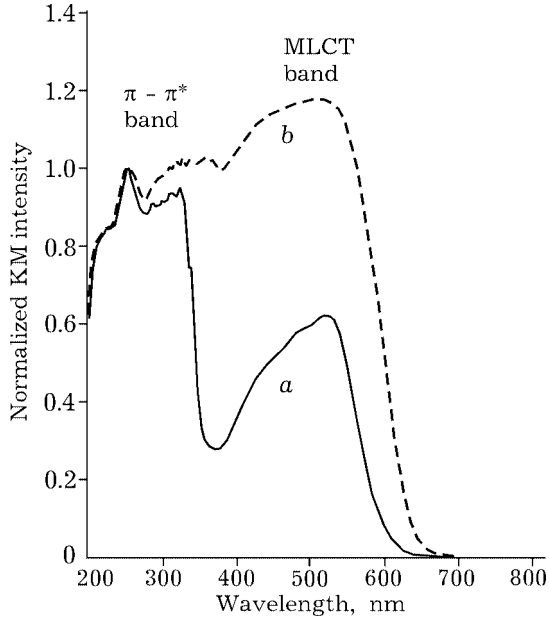


Fig. 9. UV–vis diffuse reflectance spectra of 3 min-milled mixtures comprising (*a*) phen and intact $FeCl_2 \times 4H_2O$; and (*b*) phen and preliminary 3 h-milled $FeCl_2 \times 4H_2O$.

of $FeCl_2 \times 4H_2O$ for 3 h and subsequent milling with phen for 3 min brought about almost the same reaction as we observed after milling the mixture for 3 h from the beginning without preliminary milling of $FeCl_2 \times 4H_2O$ alone. On the other hand, preliminary milling of phen alone did not bring about any change in the subsequent mechanochemical reaction with $FeCl_2 \times 4H_2O$.

## SUMMARY AND OUTLOOK FOR NEAR FUTURE

Some experimental evidences are shown how the ligand field loses its symmetry with substantial broadening of the ligand field strength as a consequence of milling crystalline metal coordination compounds. This leads to facile mechanochemical synthesis of a number of coordination compounds that are conventionally prepared via a tedious solution route. As-milled products are not always identical with those from a solution process. By annealing the milled products, we further found some anomaly. While simple recovery and recrystallization are observed in some compounds, phase transformation is often observed as well for other compounds. This brings about still new crystalline state coupled with specific spin states. A systematic study on the formation of new coordination crystals via a combination of mechanochemical and thermal processes is now ongoing.

Loss of symmetry may play much further and diverse role in solid state chemistry, only in which distorted molecules with varying degree of lower symmetry can be preserved when we deal with molecular crystals. The concept might further be extended to more complicated organic synthesis whenever this is to be done in a solid state. The procedure is quite easy and mild so that it is completely in harmony with the sustainable way of chemistry coined as green chemistry.

## ACKNOWLEDGEMENT

The present feature article is based mainly on the doctoral works of Ms. N. Tsuchiya and Mr. T. Oshita. The author sincerely thanks them for their achievement and cooperation. These studies were partly supported by the Grant-in-Aid for Scientific Researches (No. 09490033) from the Ministry of Education, Science, Sports and Culture in Japan.

## REFERENCES

1 P. W. Atkins, Physical Chemistry, 6th Ed., Oxford University Press, Oxford, 1998, p. 343.
2 M. Senna, Y. Fujiwara, T. Isobe and J. Tanaka, *Solid State Ionics*, 141–142 (2001) 31.
3 N. Tsuchiya, T. Isobe, M. Senna *et al.*, *Solid State Commun.*, 99 (1996) 525.
4 N. Tsuchiya, A. Tsukamoto, T. Ohshita *et al.*, *J. Solid State Chem.*, 153 (2000) 82.
5 O. Kahn, Molecular Magnetism, VCH, New York, 1993, p. 53.
6 P. Gütlich, Structure and Bonding, Vol. 44, Springer-Verlag, Berlin, 1981, pp. 83.
7 P. Gütlich, *J. Phys. Colloq.*, C2 (1979) 378.
8 J. E. Huheey, Inorganic Chemistry: Principles of Structure and Reactivity, 2nd Ed., Harper&Row, New York, 1978, p. 332.
9 E. W. Müller, H. Spiering and P. Gütlich, *Chem. Phys. Lett.*, 93 (1982) 567.
10 E. W. Müller, H. Spiering and P. Gütlich, *J. Chem. Phys.*, 79 (1983) 1439.
11 M. S. Haddad, W. D. Federer, M. W. Lynch and D. N. Hendrickson, *J. Am. Chem. Soc.*, 102 (1980) 1468.
12 M. S. Haddad, W. D. Federer, M. W. Lynch and D. N. Hendrickson, *Inorg. Chem.*, 20 (1981) 131.
13 N. Tsuchiya, A. Tsukamoto, T. Ohshita *et al.*, *J. Solid State Sci.*, (2001) in press.
14 M. Nakano, S. Okuno, G.-E. Matsubayashi *et al.*, *Mol. Cryst. Liq. Cryst.*, 286 (1996) 83.
15 M. Sorai and S. Seki, *J. Phys. Chem. Solids*, 35 (1974) 555.
16 B. R. Penfold and J. A. Grigor, *Acta Cryst.*, 12 (1959) 850.
17 T. Ohshita, D. Nakajima, A. Tsukamoto *et al.*, to appear.
18 K. Madeja and E. Konig, *J. Inorg. Nucl. Chem.*, 25 (1963) 377.
19 B. Hutchinson, J. Takemoto and K. Nakamoto, *J. Am. Chem. Soc.*, 92 (1970) 3335.
20 Y. Saito, J. Takemoto, B. Hutchinson and K. Nakamoto, *Inorg. Chem.*, 11 (1972) 2003.
21 D. A. Thorton and G. M. Watkins, *J. Coord. Chem.*, 25 (1992) 299.